Biophysical Journal Volume 100 June 2011 2539–2547

A Model for Segregation of Chromatin after Replication: Segregation of Identical Flexible Chains in Solution

Ron Dockhorn[†*] and Jens-Uwe Sommer[†‡]
[†]Leibniz Institute of Polymer Research Dresden, Dresden, Germany; and [‡]Technische Universität Dresden, Institute for Theoretical Physics, Dresden, Germany

ABSTRACT We study the segregation of two long chains from parallel but randomly twisted start conformations under good solvent conditions using Monte Carlo simulations to mimic chromatin segregation after replication in eukaryotic cells in the end of prophase. To measure the segregation process, we consider the center-of-mass separation between the two chains and the average square distance between the monomers which were connected before segregation starts. We argue that segregation is dominated by free diffusion of the chains, assuming that untwisting can be achieved by Rouse-like fluctuations on the length scale of a twisted loop. Using scaling analysis, we find that chain dynamics is in very good agreement with the free diffusion hypothesis, and segregation dynamics follows this scaling nearly. Long chains, however, show retardation effects that can be described by a new (to us) dynamical exponent, which is slightly larger than the dynamical exponent for Rouse-like diffusion. Our results indicate that nearly free diffusion of chains during a timescale of a few Rouse-times can lead to segregation of chains. A main obstacle during segregation by free diffusion is random twists between daughter strands. We have calculated the number of twists formed by the daughter strands in the start conformations, which turns out to be rather low and increases only with the square-root of the chain length.

INTRODUCTION

One of the most important processes of Life is the replication of DNA. To distribute the daughter strands after replication into the respective daughter cells, Nature has to resolve a physical problem: How to separate two absolutely identical, long-chain molecules. This is of particular importance for eukaryotes, where very long DNA, compactified as chromatin, have to be segregated faithfully. Here, the process leads to the formation of mitotic chromosomes, where the two strands are additionally compacted and held together by a centromere region, waiting for final separation by the spindle apparatus setup for cell-division.

The particular problem in eukaryotic cells during mitosis or meiosis is that all DNA strands have to be segregated perfectly, but stay together until cell-division starts. Failures of segregation and distribution of DNA during the cell-division are usually lethal for cells. It is important to stress that the segregation process of the conformations of the daughter chains takes place before cell-division starts, and mitotic chromosomes are structures where DNA segregation has been accomplished (1–4).

It is very likely that this segregation problem is solved based on physical principles; there is no indication for the operation of motor proteins which directionally pull the daughter strands during the chromosome formation (prophase). There is also no indication for a distinction of the daughter strands—even histones (note that additional histones have to be created during replication) which compact DNA into the chromatin fibers, using both old and new histones, are randomly distributed among the daughter strands (5,6).

Considering these facts, there remain the following driving forces for segregation: the mutual repulsion between the chain molecules, the excluded volume effect well known in polymer physics, and the random diffusion dynamics. The aim of this work is to study the segregation of two identical flexible chains starting from an identical conformational state under the action of undirected excluded volume interactions under good solvent conditions. As a first step, we simplify the actual problem by considering two strands of chromatin in the end of the prophase and investigate the properties of the segregation kinetics.

A similar problem has been addressed in the literature for the case of DNA-segregation in bacteria (7–10). By assuming that the radius of gyration of the unconstrained DNA molecules is much larger than the diameter of the tube forming the bacterial cell, a constant entropic driving force for segregation of two overlapping chains can be derived. This argument is based on scaling concepts for confined chains which are well established in the polymer literature (11,12) and has been tested in computer simulations (13–17). When the above noted ratio between free extension of DNA and tube diameter is large, the gain of free energy by segregation is large as compared to k_BT, where k_B denotes Boltzmann's constant and T is the absolute temperature. The cylindrical shape directs the segregation process, and as a result the two strands are located in opposite parts of the cell.

The situation is different during the prophase in eukaryotic cells. Here, the cell shape is not supporting a simple mechanism as assumed for tubelike prokaryotic cells.

Submitted November 16, 2010, and accepted for publication March 25, 2011.

*Correspondence: dockhorn@ipfdd.de

Editor: Laura Finzi.

0006-3495/11/06/2539/9 $2.00
doi: 10.1016/j.bpj.2011.03.053

Moreover, several DNA strands have to be separated faithfully at the same time. The simplest solution is that segregation is still driven by excluded volume repulsion between the two strands and geometric constraints may play a minor role. However, considering the thermodynamics of polymer solutions, we know that the gain in free energy between the mixed state of two polymers and the segregated state is of the order of k_BT only (11). Thus, only a very small driving force can operate between two equilibrium states (mixed and segregated state).

Simulation model and description of segregation kinetics

We assume that the segregation dynamics of the two daughter strands is driven by Brownian motion of the flexible units (segments) of chromatin in the absence of hydrodynamic interactions. This should give us a first insight into the segregation processes. Hydrodynamic effects are computationally very demanding and could be considered in later studies. Under physiological conditions (high salt content), electrostatic interactions can be neglected on the length-scale of the chromatin thickness (18–21). Therefore, we consider the model of two flexible uncharged polymer chains where the smallest relevant length scale is the Kuhn segment of the chromatin fiber, which corresponds to the length scale where conformational changes can be considered as uncorrelated. The Kuhn length can be related to the so-called persistence length, which is defined by the decorrelation length of two repeat units along the strand. In simplified models, the Kuhn length is twice the persistence length (see Rubinstein and Colby (22) for more information about chain models).

Before segregation starts, the two linear daughter chains are connected by a rope-ladder-like structure. The daughter chains correspond to chromatin fibers (thickness ~30 nm) in the end of the prophase held together by cohesin (23–25). The Kuhn length of chromatin has been estimated to ~300 nm $\triangleq$ 30 kbp (26). Thus, 1000 repeat units of our model correspond to ~30,000 kbp per chain. For comparison, one human eukaryotic chromosome with 130,000 kbp (27) would correspond to ~4000 repeat units of our model.

To simulate the segregation process we apply the bond fluctuation method (28,29). In this coarse-grained model, the repeat units are modeled as cubes occupying eight corners on a simple cubic lattice (see Fig. 1). The connectivity between the monomers is given by a set of 108 bond vectors out of permutations of six basic vectors which enable a high flexibility in the conformational state. Monte Carlo sampling is performed by successive jumps of randomly selected monomers along a randomly selected unit lattice vector by fulfilling the conditions that the targeted place is not occupied (excluded volume) and the new bond vector is within the allowed set.

The basic time unit is defined as one Monte Carlo step (*MCS*), which corresponds to one attempted monomer move in average. The set of bond vectors is chosen to preserve topological constraints during the random motion of the chains (cut-avoiding). Note that the algorithm we are using in this work corresponds to a Langevin-type dynamics of the polymer chains which displays the characteristic dynamical features of real chains in the absence of hydrodynamic interactions.

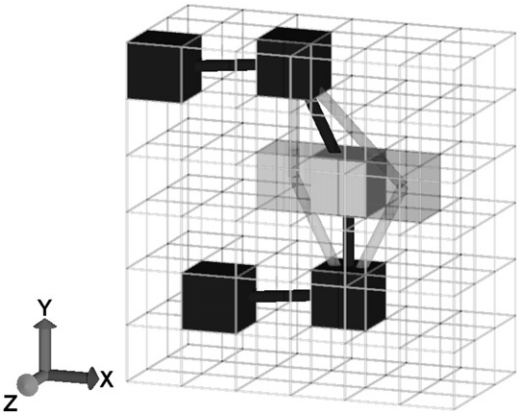

FIGURE 1 Sketch of the bond-fluctuation-model (28,29) as Monte Carlo method for simulating the chains. Repeat units are modeled as cubes occupying eight corners on a simple cubic lattice (*solid cubes*) and the connectivity between the monomers (*solid cylinder*) is given by a set of 108 bond vectors out of permutations of six basic vectors. Successive jumps of randomly selected monomers (*shaded cubes*) along a randomly selected unit lattice vector are tested for excluded volume condition and if the new bond vector is within the allowed set. The move is performed if the conditions are fulfilled (*left cube*) or rejected (*right cube* with invalid bond).

The start conformation is defined by an equilibrium conformation of two chains forming a rope ladder (connecting each monomer in both strands by additional bonds representing cohesin units) in good solvent without confinement, using periodic boundary condition for the lattice. The equilibrium state of the double-strand formed by the two daughter chains of chromatin corresponds to a self-avoiding random walk on long scales, whereas on short scales both strands are randomly twisted. The onset of the segregation process is set to the instantaneous cleavage of all interchain bonds (opening the cohesin bonds), and segregation is driven by the excluded volume repulsion of the two chains and random motion. Simulations of 100 independent runs up to 50×50^6 *MCS* are performed in a $512 \times 512 \times 512$ simulation box with periodic boundary conditions applied in all three directions, and ensemble averaging is done with respect to the onset of segregation: For all runs we have selected different start conformations of the double-strand of chromatin.

In Fig. 2, we show snapshots taken during the segregation process to illustrate the dynamics of the two chains. At the beginning, both chains are intertwined due to the initial rope-ladder-like structure. After cleavage of the interchain bonds, segregation dynamics arises from excluded volume repulsion and random motion of the chains. This process is slowed down due to initial twists between daughter strands (indicated by *red arrows* in Fig. 2). The random

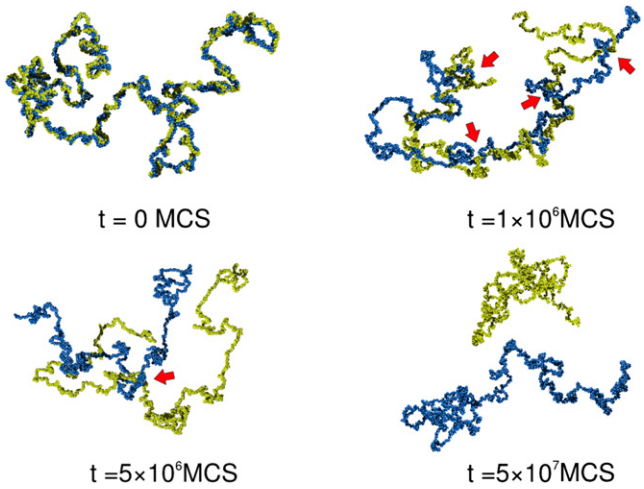

FIGURE 2 Snapshot of conformations of chains with $N = 1000$ at different times during the segregation process. At the beginning, both chains are intertwined. Segregation dynamics is slowed down due to twists between daughter strands (indicated by *red arrows*). Successive unwinding leads to two segregated strands (*color online*).

motion of both chains reduces the number of twists as segregation continues. As a result, the unwinding leads to two spatially separated strands in the end of the segregation process.

Two quantities which characterize the size of a polymer chain made of N repeat units are the mean squared end-to-end distance R_{ee}^2 and the mean-squared radius of gyration R_g^2. They are defined as

$$R_{ee}^2 = (\vec{r}_N - \vec{r}_1)^2 \tag{1}$$

and

$$R_g^2 = \frac{1}{N}\sum_{i=1}^{N}(\vec{r}_i - \vec{r}_{COM})^2, \tag{2}$$

where $\vec{r}_{COM}$ denotes the position of the center-of-mass of an individual chain and $\vec{r}_i$ denotes the position of the monomer i. All observables are averaged over independent runs (and start conformations) of the segregation process. As seen in the inset of Fig. 3 and Table 1, the start conformation is slightly stretched because additional bonds between the strands (rope-ladder-structure) increase the stiffness of the double-chain as compared to individual chains. Both quantities show a rapid initial decay due to the loss of this additional stiffness, followed by a much slower relaxation process.

Insight into the segregation dynamics can be found by analyzing the center-to-center vector between the two chains, which we denote as $\mathcal{A}/\mathcal{B}$ in the following:

$$\vec{R}_{c2c}(t) = \vec{r}_{COM,\mathcal{B}}(t) - \vec{r}_{COM,\mathcal{A}}(t). \tag{3}$$

Usually, the norm of the center-to-center vector

$$R_{c2c} = |\vec{R}_{c2c}|$$

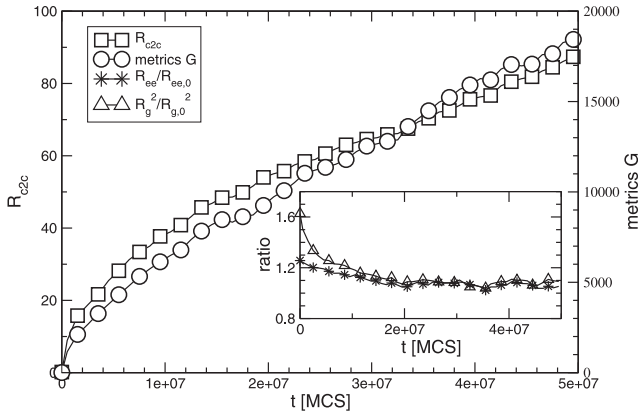

FIGURE 3 Center-to-center distance R_{c2c} and metrics G for two chains of length $N = 1000$ during segregation. (*Inset*) Ratios of end-to-end distance R_{ee}, and radius of gyration R^2_g, compared to an unconstrained chain.

will be evaluated. The center-of-mass of a polymer chain is defined by

$$\vec{r}_{COM} = \frac{1}{N}\sum_{k=1}^{N}\vec{r}_k.$$

Furthermore, we define the integral distance (metrics) between the chains according to

$$G(t) = \frac{1}{N}\sum_{i=1}^{N}(\vec{r}_{\mathcal{A},i}(t) - \vec{r}_{\mathcal{B},i}(t))^2. \tag{4}$$

The center-to-center distance $R_{c2c}(t)$ gives overall information about the relative position of the two chains in space. Different from that, the metrics $G(t)$ describes the averaged distance of two initial adjacent monomers of different chains and provides local information of the segregation process by using the local position of two functions $\vec{r}_{\mathcal{A}/\mathcal{B}}(t)$. Formally, it corresponds to a distance in the metrical space of chain conformations ($3N$-dimensional). An example for the behavior of both quantities for chains of length $N = 1000$ is displayed in Fig. 3. At initial timescales ($t \lesssim 3 \times 10^6$ *MCS*) there is a rapid increase of both observables due to the instantaneous strong interchain repulsion (excluded volume) of adjacent monomers of the daughter chains. We note that this nonequilibrium effect is caused by the strong entropic reduction which, in turn, is due to the strict parallel alignment of the two daughter chains. Formally, it

TABLE 1 End-to-end distance R_{ee}, radius of gyration R_g^2, and Rouse time τ_R for a single linear chain ($N = 1000$) and a double-strand (rope-ladder-structure with $N = 1000$ per strand) without perturbations

	Linear chain	Double strand
R_{ee}	159.98 ± 1.61	201.50 ± 3.58
R_g^2	4642.0 ± 48.3	7797.62 ± 234.3
τ_R	7.77×10^6 *MCS* ± 1.2×10^4 *MCS*	1.43×10^7 *MCS* ± 1.9×10^5 *MCS*

corresponds to the constraint of a narrow tube for one chain (see also *left part* of Fig. 4). This rapid process is following a slower but steady increase of both observables.

Calculation of twist number of double-strands

The twist number is a property of the initial starting conformation before cleavage of the interchain bonds of the double strand. To calculate the twist, we follow the method proposed by White and Bauer (30). For calculating the twist of strand $\mathcal{A}$ with respect to $\mathcal{B}$, denoted by $Tw(\mathcal{A}, \mathcal{B})$, we assume that both strands do not intersect, and every monomer on $\mathcal{A}$ is uniquely linked to a corresponding monomer on $\mathcal{B}$. These prerequisites are fulfilled within the simulation method due to the excluded-volume constraints, and the interchain connections between the strands.

Next, we convert the discrete monomer position information of the chains into smooth and differentiable curves by interpolating with cubic splines. (For illustration of the defined vectors, see Fig. 5.) Let $\vec{z}_{\mathcal{AB}}$ be the vector between the point a on $\mathcal{A}$ connecting to the corresponding point b on curve $\mathcal{B}$, and $\vec{t}_{\mathcal{A}}$ the unit tangent vector of the curve $\mathcal{A}$ at point a as evaluated by numerical differentiation.

Because of excluded volume constraints the vectors $\vec{z}_{\mathcal{AB}}$ and $\vec{t}_{\mathcal{A}}$ are not collinear to each other, however, they are necessarily orthogonal. Therefore, we define the unit vector $\vec{v}_{\mathcal{AB}}$ as the projected vector directed along the component of $\vec{z}_{\mathcal{AB}}$ that is perpendicular to $\vec{t}_{\mathcal{A}}$. The change $d\vec{v}_{\mathcal{AB}}$ of $\vec{v}_{\mathcal{AB}}$ is evaluated numerically and the local contribution to the twist at point a is given by

$$[\vec{t}_{\mathcal{A}} \times \vec{v}_{\mathcal{AB}}] \cdot d\vec{v}_{\mathcal{AB}}.$$

The total twist of curve $\mathcal{B}$ about $\mathcal{A}$ in number of turns is given by the formula (30)

$$Tw(\mathcal{A}, \mathcal{B}) = \frac{1}{2\pi} \int_{\mathcal{A}} [\vec{t}_{\mathcal{A}} \times \vec{v}_{\mathcal{AB}}] \cdot d\vec{v}_{\mathcal{AB}}. \quad (5)$$

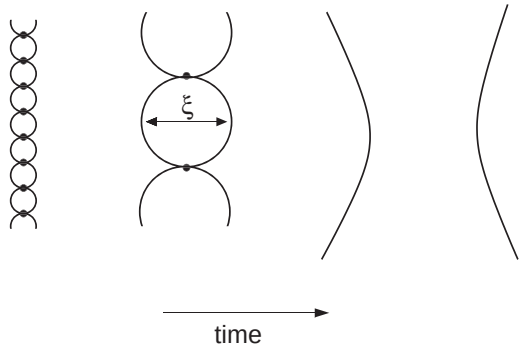

FIGURE 4 Sketch of the segregation process. Twisting is illustrated by nodes which subdivide the chains into blobs comprising g segments. As a consequence, the conformations are restricted to a tube of diameter ξ, which corresponds to the correlation length of a blob formed by a part of the chain according to $g \sim \xi^{1/\nu}$. As time proceeds, the blobs enlarge and the driving force for segregation decreases.

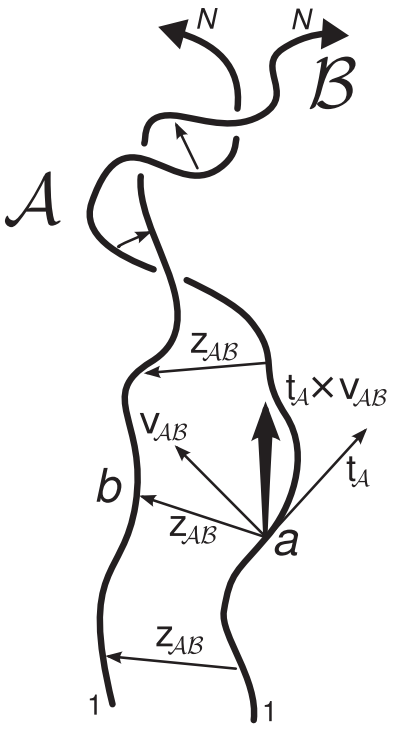

FIGURE 5 Scheme of vector definitions used for the calculation of the twist number $Tw(\mathcal{A}, \mathcal{B})$. The vector $\vec{z}_{\mathcal{AB}}$ connects the point a on $\mathcal{A}$ with the corresponding point b on curve $\mathcal{B}$. The symbol $\vec{t}_{\mathcal{A}}$ denotes the unit tangent vector of the curve $\mathcal{A}$ at point a. The unit vector $\vec{v}_{\mathcal{AB}}$ is the projected vector directed along the component of $\vec{z}_{\mathcal{AB}}$ that is perpendicular to $\vec{t}_{\mathcal{A}}$. Thus, the orthogonal basis $\vec{t}_{\mathcal{A}}$, $\vec{v}_{\mathcal{AB}}$, and $[\vec{t}_{\mathcal{A}} \times \vec{v}_{\mathcal{AB}}]$ contains the geometrical information for calculating the twist $Tw(\mathcal{A}, \mathcal{B})$ of curve $\mathcal{B}$ about $\mathcal{A}$.

Due to the symmetry between the chains in our case, the average twist of curve $\mathcal{B}$ about $\mathcal{A}$ equals the average twist of curve $\mathcal{A}$ about $\mathcal{B}$, which is not necessarily fulfilled in general. We define the average twist for different double-strands in their equilibrium state according to

$$Tw(N) = \sqrt{\langle Tw^2(\mathcal{A}, \mathcal{B}) \rangle}. \quad (6)$$

The results for our simulated double-strands are shown in Fig. 6. If we consider the evolution of twists as a random walk on a unit-circle, we expect

$$Tw^2(N) = D_{Tw} N, \quad (7)$$

where D_{Tw} denotes the intensity of random twisting. This behavior is well observed in Fig. 6. The best fit to Eq. 7 is indicated by a solid line. For the simulated system with $N = 1000$, we found an average twist of 5.3 turns between the initial conformations. By mapping this result back to the biological units, we obtain ~5 turns for chromatin of length $\simeq$300 nm and ~11 turns for a human genome of length of 1.3 mm. We note that the random twisting process is universal in a sense that all chain models with the same

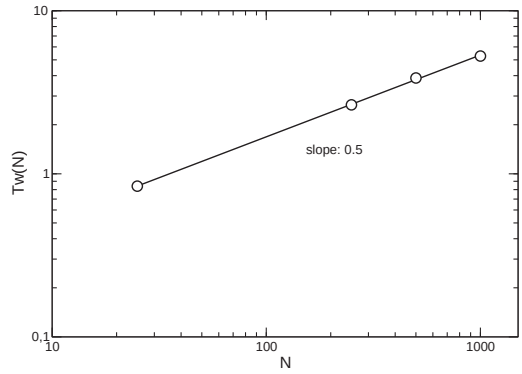

FIGURE 6 Calculated averaged twist number $Tw(N)$ for different chain lengths N. (*Solid line*) Best fit to Eq. 7 with $D_{Tw} = 0.028$.

number of Kuhn segments display the same averaged twisting number.

Kinetic models for chain segregation in good solvent

The free segregation of the daughter chains in solution is driven by excluded volume interactions and diffusion. At the beginning of the process, after cleavage of the bonds between the chains, every monomer interacts strongly with its immediate counterpart on the other chain. When separation is proceeding, interactions between monomers decrease and thus the driving force for segregation. During segregation, twisting of conformations restricts the free motion of the chains. On the other hand, for chains in good solvent, the number of entanglements shall be negligible at the overlap concentration c^*, which corresponds to two chains sharing the same volume of gyration (11).

We note that, even under poor solvent conditions, the pervaded volume as shared by only two chains is quite different from a melt state, in which many chains ($\sim N^{1/2}$) share the same volume of gyration, causing a high number of entanglements. Technically, two chains collapsed together can be mapped into two Hamiltonian walks (occupying space densely). It has been shown recently that segregation effects of both chains can observed as well (31). Even for poor solvent conditions, it is not clear whether significant entanglement constraints between only two chains arise and hinder the segregation process substantially.

Let us assume that, at a given stage of segregation, the free energy of the both chains is given by a mutual confinement to a size ξ, which indicates the average distance between the chains according to

$$F(\xi) \sim \frac{N}{g(\xi)}, \tag{8}$$

where $g(\xi)$ denotes the number of monomers within a blob defined by $g \sim \xi^{1/\nu}$, where $\nu \simeq 3/5$ is the Flory exponent of flexible chains in good solvent (11). In Fig. 4, we illustrate this by indicating the twists as nodes and the chain parts in-between as loops. We assume energy units according to $k_BT = 1$ in the following. We note that the free energy excess per blob is of order unity (k_BT). The driving force is quickly decaying, according to $f \sim \xi^{-1/\nu-1}$. Therefore, the excluded volume repulsion has small impact on the fluctuation dynamics of the loops. This is in marked contrast to the segregation of chains in a tube (7,8), where the driving force (and the blob size) is constant, leading to a constant segregation velocity (under the condition of tubelike constraints for all chain parts) which, in turn, exceeds diffusional motion on longer timescales.

In this case, fluctuations of the loops can release the twists and enlarge the length scale ξ. Let us assume that twists can be disentangled without a cooperative motion of the whole chain. To untwist a node, fluctuations of the loop of the order of its own size are necessary. This corresponds to a time $t_g \sim g^{2\nu+1}$, where we have used the dynamic exponent of free chains in solution without hydrodynamic interactions. The segregation (or untwisting) time of the chains is thus dominated by the process to untwist the largest loop and is given by

$$t_S \sim N^{2\nu+1} \sim t_R. \tag{9}$$

Thus, the segregation time is proportional to the relaxation time of the single chain in solution in the absence of hydrodynamic friction denoted as Rouse time, t_R, in the following. Hence, dynamic scaling for free chains should also hold for segregation of chains in solution. This is a direct consequence of our assumption that untwisting does not need a correlated motion of nodes. The segregation dynamics for the metrics, G, is then given by the dynamic scaling relation:

$$G(t) \sim R_0^2 \times f_G(t/t_S) \overset{t \ll t_S}{\sim} t^{2\nu/(2\nu+1)} \sim t^{6/11}. \tag{10}$$

Here, metrics $G(t)$ is assumed to be a function of time $f_G(t/t_S)$ and a function of a squared distance on the relevant length scale that is the extension of the free chain $R_0 \sim N^{\nu}$ in solution. The function $f_G(t/t_S)$ has to be a power law to fulfill the condition that for times $t >> t_S$ (segregation is complete), the function $G(t)$ behaves diffusively, and for times $t << t_S$, the incoherent movement of the nodes is independent of the chain length N. Hence, dynamic scaling yields

$$\begin{aligned} G(t) &\sim R_0^2 \times f_G(t/t_S) \sim N^{2\nu} \times t^m \times t_S^{-m} \\ &\sim N^{2\nu} \times t^m \times N^{-m(2\nu+1)} \overset{t \ll t_S}{\rightarrow} N^0 \times \tilde{f}(t). \end{aligned}$$

Thus, the latter relation is fulfilled for

$$m = \frac{2\nu}{2\nu+1} \sim 6/11$$

and yields Eq. 10. Following our model that unwinding is controlled by Rouse-like dynamics, the center-of-mass displacement of both chains scales as for single chains. Hence we expect

$$R_{c2c} \sim \frac{t}{N}. \tag{11}$$

For the case of fully unconstrained segregation (no correlations or additional friction effects), the metrics and the displacement of the center-of-mass of both chains are directly related to the single-chain displacement functions defined as

$$\begin{aligned} g_1(t) &= \frac{1}{N}\sum_{k=1}^{N}\left\langle[\vec{r}_k(t)-\vec{r}_k(0)]^2\right\rangle \\ &\text{and} \\ g_3(t) &= \left\langle[\vec{r}_{COM}(t)-\vec{r}_{COM}(0)]^2\right\rangle, \end{aligned} \tag{12}$$

where the brackets denote the average over independent start conformations. In Fig. 7, the relation between single-chain and relative displacements of monomers is sketched. If we denote an arbitrary displacement vector by $x_{\mathcal{AB}}$, we obtain

$$\left\langle x_{\mathcal{AB}}^2\right\rangle = 2\left\langle x^2\right\rangle - 2\langle x_{\mathcal{A}} \cdot x_{\mathcal{B}}\rangle, \tag{13}$$

where x refers to either chain by symmetry. For ideal segregation, the center-of-mass diffusion of both chains is fully uncorrelated and the following relation must hold for all timescales:

$$R_{c2c}(t) = 2 \times g_3(t). \tag{14}$$

The relation between $G(t)$ and $g_1(t)$ is less obvious because the chains share exactly the same start conformation, which impacts the relative motion due to the nonzero memory function of the monomer displacements. For Rouse dynamics (without excluded volume effects), one obtains exactly

$$G(t) = g_1(2t). \tag{15}$$

Moreover, single-chain displacement functions show scaling behavior with a scaling function, f, according to

$$g_k(t)/R_0^2 = f_k(t/t_R), \tag{16}$$

a property which is transferred to $G(t)$ and $R_{c2c}(t)$ in the case of ideal segregation. Effects of twisting (retardation of segregation) and excluded volume repulsion (acceleration of segregation) will lead to deviations from these results. As discussed above, the latter effect should only be important on short timescales.

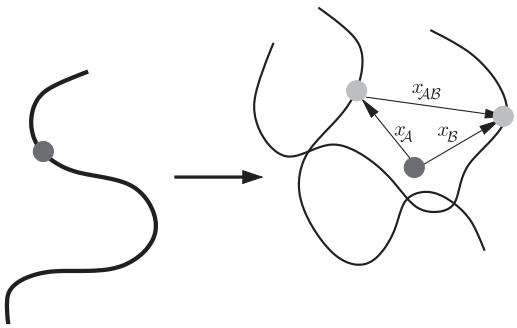

FIGURE 7 Sketch of the single chain and relative displacements of monomers during segregation.

A comparison of the segregation process with the dynamics of free chains is shown in Fig. 8. Here, we display the metrics, the g_1-functions of individual chains during segregation, as well as the g_1-function of a single chain in good solvent (free). The relations for ideal segregation, Eqs. 15 and 16, are applied to rescale the data. As a reference system, we used $N = 1000$ (for $N = 1000$ all time- and length-scales correspond to the simulated time- and length-scales). We note that all g_1-functions obey perfect scaling. Thus, segmental motion during segregation is the same as in free solution. The dynamic exponents of $2\nu/(2\nu + 1) \simeq 6/11$ for $t << t_R$, and of 1 for $t >> t_R$, are reproduced as indicated by the dashed-dotted lines in Fig. 8. The crossing of both lines can be used to define the segregation time t_S, which coincides with a mean-squared displacement of $4 \times R^2{}_g$. We obtain

$$t_S(N = 1000) \sim t_R(N = 1000) \simeq 10^8\ MCS.$$

Very good agreement between the metrics and single-chain displacements according to Eq. 15 is obtained for short chains, $N = 25$. Acceleration at very short times (~100–1000 *MCS* in unscaled units), as compared to free fluctuations, is obtained for all chain lengths. At early stages of segregation, excluded volume repulsion between the chains explains this behavior. Due to rescaling of the data in Fig. 8, this effect is most visible for the shortest chains. For longer chains, we observe a retardation in the Rouse-regime $t < t_R$. Here, segregation dynamics is slowed down as compared to free chain dynamics. Crossover to free

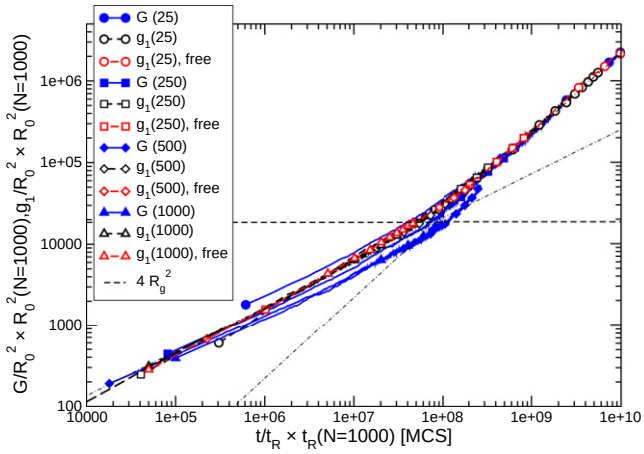

FIGURE 8 Comparison of the metrics and single chain displacement functions for various chain lengths. Rouse-scaling is applied with respect to the reference system $N = 1000$ according to Eq. 16. The data for $G(t)$ are shifted in time by a factor of two according to Eq. 15. (*Dashed-dotted lines*) Expected slopes of 6/11 and 1, respectively. The segregation time and the related Rouse time can be estimated by the crossing of the two lines.

dynamics takes place in the range of t_R. For the longest chains, $N = 500$, $N = 1000$, we clearly observe $t_S > t_R$. We note that the results for $N = 1000$ does not display a crossover to free diffusion up to the maximum simulation time.

Complementary to the monomer segregation described by the metrics and shown in Fig. 9, we have plotted the mean-square displacement between the center-of-mass of both chains, $R_{c2c}(t)$, using Rouse-scaling with respect to the reference system $N = 1000$. The data for free diffusion are located on the dotted line and are not shown. The dashed line indicates the ideal segregation dynamics as predicted in Eq. 14. Again, the data for $N = 25$ displays good convergence. The excluded volume-driven acceleration at the beginning of the segregation process is more pronounced as compared to the segmental motion in Fig. 8. The data for long chains again display retardation effects in the Rouse-regime. Here an effective slope of ~0.85 can be fitted to the data for $N = 500$, 1000. This would indicate a subdiffusive behavior in some contrast to ideal segregation.

These observations of a retardation behavior for segregating chains as compared to free chain dynamics might suggest a new dynamical exponent related to segregation of chains in good solvent. We generalized Eq. 9 to

$$t_S \sim N^{\omega}, \tag{17}$$

where ω denotes the new dynamical exponent. Dynamic scaling according to Eq. 16 and independence of $G(t)$ from the chain length for $t << t_S$ (which is well obeyed for the unscaled data of Fig. 8) leads to

$$G(t) \sim t^{2\nu/\omega}. \tag{18}$$

Best fit for the data for long chains yields $2\nu/\omega \simeq 0.5$, and thus, $\omega \simeq 4\nu$. These results are tested in the scaling plot of Fig. 10. Better agreement is achieved between the data for long chains as compared to Figs. 8 and 9.

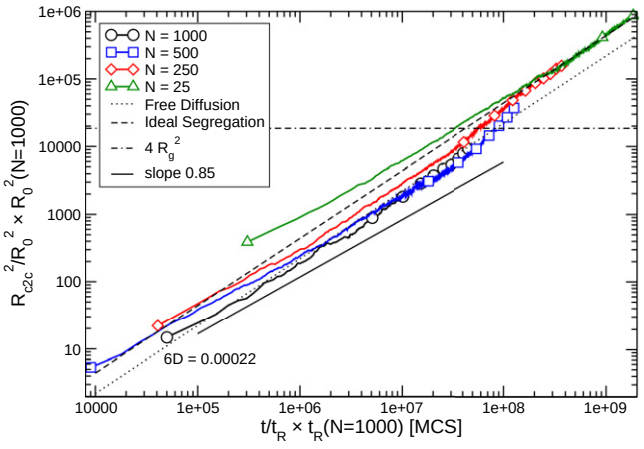

FIGURE 9 Mean-square displacement of the center-of-mass of both chains. Rouse-scaling is applied with respect to the reference system $N = 1000$. The data for free diffusion all coincide on the dotted line (not shown).

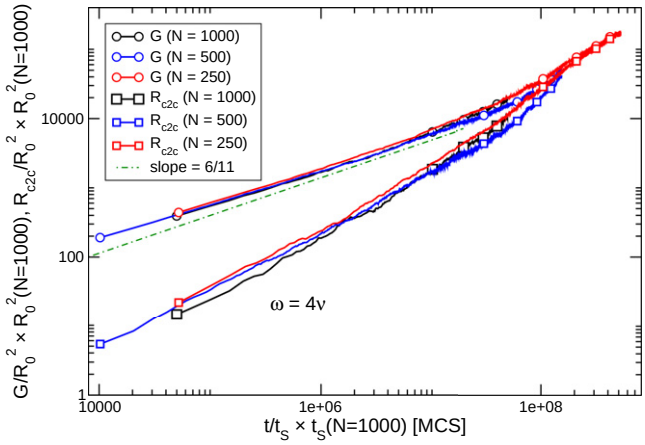

FIGURE 10 Scaling plot using a dynamical scaling exponent $\omega = 4\nu$ as obtained from the effective slope of $G(t)$.

The origin for nonideal segregation lies in the assumption about uncorrelated untwisting which will be not fulfilled for long chains. To resolve an overall twist of the chains, cooperative untwisting events may be necessary which lead to longer timescales. This process reminds us of the reptation problem in polymer melts. In fact, sliding along the contour of both chains could release the twisting constraints. However, this is not observed in our simulation, and does not fit to the natural process. In the latter, both daughter strands are connected by the centromere at the final stage of the segregation. The natural process might even suggest that the central regions of both strands are not segregating. Thus, the dynamical process which resolves twisting constraints between two polymer chains, and which leads to the deviation from ideal segregation behavior, might correspond to what we consider a new type of polymer dynamics.

CONCLUSIONS AND OUTLOOK

We have analyzed the segregation dynamics of two identical flexible chains in good solvent. In particular, we have considered the following simple argument: When the chains are diluted in a good solvent, entanglement constraints should be of minor importance. On the other hand, if two chain conformations are very close, twisting can be a major obstacle for segregation and has to be resolved. The average time to untwist a chain on a length scale ξ corresponds to the (Rouse) time associated with random fluctuations on that scale. On average, one fluctuation mode of length ξ is necessary to untwist. However, it is assumed that no cooperative motion is necessary to untwist the chains on larger scales. This results exactly in the free diffusion scaling, and the segregation functions should obey the corresponding dynamic scaling.

To test our assumptions, we have considered two measures for segregation: The metrics, $G(t)$, which corresponds to the

averaged monomer displacement function for single chain dynamics; and the center-to-center displacement, R_{c2c}, which corresponds to the center-of-mass displacement in single chain dynamics.

We found that the free diffusion concept for chain segregation is obeyed for shorter chains and scaling using the Rouse time is roughly obeyed. Moreover, the diffusion functions g_1 and g_3 of the individual chains during segregation do not deviate from those of single chains in dilute solution. Stronger deviations from the free diffusion behavior occur for longer chains. Here, the concept of uncorrelated untwisting of the chains may be not valid. Better agreement with the simulation data is obtained if a new dynamical exponent, $\omega \simeq 4\nu > 1 + 2\nu$, is introduced. For the longest chains there is a factor of ~3–4 between Rouse-time and the segregation time predicted by the new dynamical exponent. Thus, segregation time can be considered to be of the order of the Rouse time for free diffusion. The average number of twists between two chains of length 1000 is ~5—thus, not very high, and it is growing with a square-root of the chain length only. Therefore, twisting shall not be a major obstacle for segregation.

We shall note that dynamics of untwisting of two chains, to the best of our knowledge, has not been considered theoretically before. The emergence of a new dynamical exponent is thus not surprising. For a more quantitative and analytical study, however, larger systems and longer timescales have to be studied.

The interesting question is whether in principle the Rouse time could be the characteristic timescale for DNA-segregation in eukaryotes. Comparing the diffusion coefficient for interphase chromosome of *Drosophila* spermatocytes (32) and human chromatin (33) with the simulation time yields a segregation time between several hours and a few days. The total cell-cycle time in most animal cells often lasts between 12 and 24 h with <1 h for the M-phase (1). Thus, the segregation process seems to be quicker, although the corresponding timescale is of the same order of magnitude as the Rouse time.

Even if the concept of free diffusion can nearly explain the segregation process, there are still some open issues:

1. Segregation should be perfectly accomplished (not just in average) even under the restriction that both daughter-strands stay close to each other.
2. The role of condensin has to be understood. Condensin is a protein complex formed by SMC (structural maintenance of chromosomes) ATPase subunits that can bind to DNA and hydrolyze ATP. These evolutionary conserved proteins are essential to compact chromatin fibers into metaphase chromosomes, but the exact mechanism is still unclear (23,34–36). It has been shown that condensin is vital for the proper formation of chromosomes and a successfully accomplished cell cycle.
3. A large amount of entropy is apparently wasted because the strong conformation restrictions of both chains at the beginning is not used to control segregation. Here, the role of another SMC protein complex, known as cohesin, at the beginning of the segregation process is unclear. It establishes sister chromatid cohesion during the S-phase lasting until prometaphase and the final release at the centromere region in late anaphase (36–38).

Further work is in progress to clarify some of these issues.

REFERENCES

1. Alberts, B., A. Johnson, …, P. Walter. 2002. Molecular Biology of the Cell, 4th Ed. Garland Science, New York.
2. Lodish, H. F., M. Scott, …, M. Krieger. 2003. Molecular Cell Biology, 5th Ed. W. H. Freeman, New York.
3. Berg, J. M., J. L. Tymoczko, and L. Stryer. 2002. Biochemistry, 5th Ed. W. H. Freeman, New York.
4. Koshland, D., and A. Strunnikov. 1996. Mitotic chromosome condensation. *Annu. Rev. Cell Dev. Biol.* 12:305–333.
5. Jackson, V., and R. Chalkley. 1981. A new method for the isolation of replicative chromatin: selective deposition of histone on both new and old DNA. *Cell.* 23:121–134.
6. Groth, A. 2009. Replicating chromatin: a tale of histones. *Biochem. Cell Biol.* 87:51–63.
7. Jun, S., and B. Mulder. 2006. Entropy-driven spatial organization of highly confined polymers: lessons for the bacterial chromosome. *Proc. Natl. Acad. Sci. USA.* 103:12388–12393.
8. Arnold, A., and S. Jun. 2007. Time scale of entropic segregation of flexible polymers in confinement: implications for chromosome segregation in filamentous bacteria. *Phys. Rev. E Stat. Nonlin. Soft Matter Phys.* 76:031901.
9. Stavans, J., and A. Oppenheim. 2006. DNA-protein interactions and bacterial chromosome architecture. *Phys. Biol.* 3:R1–R10.
10. Sherratt, D. J. 2003. Bacterial chromosome dynamics. *Science.* 301:780–785.
11. DeGennes, P.-G. 1979. Scaling Concepts in Polymer Physics. Cornell University Press, New York.
12. Brochard, F., and P.-G. DeGennes. 1977. Dynamics of confined polymer chains. *J. Chem. Phys.* 67:52–56.
13. Milchev, A., and K. Binder. 1996. Dynamics of polymer chains confined in slit-like pores. *J. Phys. II.* 6:21–31.
14. Sheng, Y., and M. Wang. 2001. Statics and dynamics of a single polymer chain confined in a tube. *J. Chem. Phys.* 114:4724–4729.
15. Chen, S. B. 2005. Monte Carlo simulations of conformations of chain molecules in a cylindrical pore. *J. Chem. Phys.* 123:074702.
16. Jun, S., D. Thirumalai, and B.-Y. Ha. 2008. Compression and stretching of a self-avoiding chain in cylindrical nanopores. *Phys. Rev. Lett.* 101:138101.
17. Arnold, A., B. Bozorgui, …, S. Jun. 2007. Unexpected relaxation dynamics of a self-avoiding polymer in cylindrical confinement. *J. Chem. Phys.* 127:164903.
18. Münkel, C., and J. Langowski. 1998. Chromosome structure predicted by a polymer model. *Phys. Rev. E Stat. Phys. Plasmas Fluids Relat. Interdiscip. Topics.* 57:5888–5896.
19. Emanuel, M., N. H. Radja, …, H. Schiessel. 2009. The physics behind the larger scale organization of DNA in eukaryotes. *Phys. Biol.* 6:025008.
20. Odenheimer, J., D. W. Heermann, and G. Kreth. 2009. Brownian dynamics simulations reveal regulatory properties of higher-order chromatin structures. *Eur. Biophys. J.* 38:749–756.
21. Gagliardi, L. 2005. Electrostatic force generation in chromosome motions during mitosis. *J. Electrost.* 63:309–327.

22. Rubinstein, M., and R. Colby. 2003. Polymer Physics. Oxford University Press, New York.

23. Hirano, T. 2002. The ABCs of SMC proteins: two-armed ATPases for chromosome condensation, cohesion, and repair. *Genes Dev.* 16: 399–414.

24. Nasmyth, K. 2002. Segregating sister genomes: the molecular biology of chromosome separation. *Science.* 297:559–565.

25. Nasmyth, K., and C. H. Haering. 2005. The structure and function of SMC and kleisin complexes. *Annu. Rev. Biochem.* 74:595–648.

26. Ostashevsky, J. Y., and C. S. Lange. 1994. The 30 nm chromatin fiber as a flexible polymer. *J. Biomol. Struct. Dyn.* 11:813–820.

27. Bielka, H., and T. Börner. 1995. Molecular Biology of the Cell [*Molekulare Biologie der Zelle*]. Gustav Fischer Verlag, Jena, Germany.

28. Carmesin, I., and K. Kremer. 1988. The bond fluctuation method: a new effective algorithm for the dynamics of polymers in all spatial dimensions. *Macromolecules.* 21:2819–2823.

29. Deutsch, H., and K. Binder. 1991. Interdiffusion and self-diffusion in polymer mixtures: a Monte Carlo study. *J. Chem. Phys.* 94:2294–2304.

30. White, J. H., and W. R. Bauer. 1986. Calculation of the twist and the writhe for representative models of DNA. *J. Mol. Biol.* 189:329–341.

31. Jacobsen, J. L. 2010. Demixing of compact polymers chains in three dimensions. *Phys. Rev. E Stat. Nonlin. Soft Matter Phys.* 82:051802.

32. Vazquez, J., A. S. Belmont, and J. W. Sedat. 2001. Multiple regimes of constrained chromosome motion are regulated in the interphase *Drosophila* nucleus. *Curr. Biol.* 11:1227–1239.

33. Chubb, J. R., S. Boyle, …, W. A. Bickmore. 2002. Chromatin motion is constrained by association with nuclear compartments in human cells. *Curr. Biol.* 12:439–445.

34. Hirano, T. 2005. Condensins: organizing and segregating the genome. *Curr. Biol.* 15:R265–R275.

35. Hirano, M., and T. Hirano. 2006. Opening closed arms: long-distance activation of SMC ATPase by hinge-DNA interactions. *Mol. Cell.* 21:175–186.

36. Hirano, T. 2006. At the heart of the chromosome: SMC proteins in action. *Nat. Rev. Mol. Cell Biol.* 7:311–322.

37. Losada, A., and T. Hirano. 2005. Dynamic molecular linkers of the genome: the first decade of SMC proteins. *Genes Dev.* 19:1269–1287.

38. Shintomi, K., and T. Hirano. 2007. How are cohesin rings opened and closed? *Trends Biochem. Sci.* 32:154–157.